Probing the conformal Calabrese-Cardy scaling with cold atoms

J. Unmuth-Yockey, Jin Zhang, P. M. Preiss, Li-Ping Yang, S.-W. Tsai, and Y. Meurice

Phys. Rev. A **96**, 023603 — Published 1 August 2017

DOI: 10.1103/PhysRevA.96.023603

Probing the conformal Calabrese-Cardy scaling with cold atoms

J. Unmuth-Yockey[1], Jin Zhang[2], P. M. Preiss[3], Li-Ping Yang[4], S.-W. Tsai[2], and Y. Meurice[1]
[1] *Department of Physics and Astronomy, The University of Iowa, Iowa City, IA 52242, USA*
[2] *Department of Physics and Astronomy, University of California, Riverside, CA 92521, USA*
[3] *Physikalisches Institut, Heidelberg University, 69120 Heidelberg, Germany and*
[4] *Department of Physics,Chongqing University, Chongqing 401331, China*
(Dated: July 14, 2017)

We demonstrate that current experiments using cold bosonic atoms trapped in one-dimensional optical lattices and designed to measure the second-order Rényi entanglement entropy S_2, can be used to verify detailed predictions of conformal field theory (CFT) and estimate the central charge c. We discuss the adiabatic preparation of the ground state at half-filling and small hopping parameter J/U, where we expect a CFT with $c = 1$. We provide two complementary methods to estimate and subtract the classical entropy generated by the experimental preparation and imaging processes. We compare numerical calculations for the classical O(2) model with a chemical potential on a 1+1 dimensional lattice, and the quantum Bose-Hubbard Hamiltonian implemented in the experiments. S_2 is very similar for the two models and follows closely the Calabrese-Cardy scaling, $(c/8)\ln(N_s)$, for N_s sites with open boundary conditions, provided that the large subleading corrections are taken into account.

PACS numbers: 05.10.Cc, 11.15.Ha, 11.25.Hf, 37.10.Jk, 67.85.Hj, 75.10.Hk

I. INTRODUCTION

The concept of universality provides a unified approach to the critical behavior of lattice models studied in condensed matter, lattice gauge theory (LGT) and experimentally accessible systems of cold atoms trapped in optical lattices. Conformal field theory (CFT) [1, 2] offers many interesting examples of universal behavior that can be observed for lattice models in two [3–5], three [6], and four [7, 8] dimensions. Practical simulations for these models unavoidably involve a finite volume that breaks explicitly the conformal invariance. However, this symmetry breaking follows definite patterns dictated by the restoration of the symmetry at infinite volume and allows us to identify the universality class. In view of the rich collection of interesting CFTs, it would be highly desirable to study their universality classes using quantum simulations. In order to start this ambitious program, one needs a simple concrete example to demonstrate the feasibility of the idea.

In this article, we propose to use the setup of ongoing cold atom experiments to quantum simulate the O(2) model with a chemical potential and check the predictions of CFT for the growth of the entanglement entropy with the size of the system corresponding to the universality class of the superfluid (SF) phase. The O(2) model is an extension of the Ising model where the spin is allowed to move on a circle, making an angle θ with respect to a direction of reference. This is briefly reviewed at the beginning of Sec. II. This model can be used to describe easy plane ferromagnetism and the compactness of θ leads to topological configurations called vortices. Their unbinding provides a prime example of a Berezinski-Kosterlitz-Thouless transition [9, 10] in a way that has also been advocated to apply for gauge theories near the boundary of the conformal window [11]. When space and Euclidean time are treated isotropically, this model has important common features with models studied numerically in LGT to describe relativistic systems in the continuum limit. The O(2) model is not strictly speaking a lattice gauge theory, however it is the zero coupling limit of the Abelian Higgs model in the sense defined in Ref. [32]. It would not be difficult to extend the procedure proposed here to related lattice gauge theory models. Quantum simulating this model and studying experimentally the CFT predictions would be a crucial first step towards applying similar methods for LGT models.

In the following, we show that these goals can be achieved by measuring the entanglement entropy of a simple Bose-Hubbard (BH) model in a very specific region for the adjustable couplings. The entanglement entropy measures the correlations between degrees of freedom in different regions of a system, is an important tool [12] in assessing the phase structure and the finite-size scaling. For a CFT in one space and one time (1+1) dimension, the ground state entanglement entropy increases logarithmically with the spatial volume of the system and its subsystems [12–17]. Using basic CFT results, Calabrese and Cardy [14] established that the coefficient of proportionality is in general the central charge multiplied by a rational number depending on the type of entropy and the boundary conditions (CC scaling). The central charge, denoted c, is of primordial importance in CFT. It characterizes the universality class and is present in a variety of physical observables [2, 14].

It has been proposed to use a quantum gas microscope to study the second-order Rényi entropy S_2 of one-dimensional fermionic Hubbard chains [18, 19] at half(quarter)-filling which seem consistent with $c = 1(2)$. S_2 is a measure of the departure from purity ($\hat{\rho}^2 \neq \hat{\rho}$) for a reduced density matrix and is defined in Sec. III. Recently, manipulations of twin copies of small one-

dimensional chains of cold bosonic ^{87}Rb atoms trapped in optical lattices have allowed experimental measurements of S_2 [20, 21] using a beam splitter method [22, 23]. In these experiments, the SF phase is reached by increasing the hopping parameter J to values having the same order of magnitude as the onsite energy U. It is important to realize that in order to see a clear correspondence between the BH and O(2) model, one needs $J/U \ll 1$. Some examples are given below. However, the feasibility of the measurements is restricted by the fact that very small values of J can be problematic because of disorder or finite-temperature effects. We argue that a reasonable compromise is to take $J/U \simeq 0.1$. In this regime, it is shown in the Appendix and in a more detailed study [24] that the finite size scaling is easier to resolve near half-filling. Note that for bosons, *half-filling* means twice more sites than particles, while for spin-1/2 fermions it means one particle per site.

The fits of numerical values of S_2 at half-filling are presented in Sec. III. Experimental measurements have been performed for small chains of four [20] and six [21] atoms and only slightly larger sizes are expected to be within experimental reach in the near future. In the discussion we focus on experiments with 16 sites or less. An important feature of S_2 with open boundary conditions [24] is that the subleading corrections are large and decay slowly with N_s (see Eq. (6) below). Knowing these corrections is essential to extract the leading CC scaling using N_s accessible in experiments.

In Sec. IV, we discuss the experimental setup to reach adiabatically the ground state at half-filling. We then discuss methods to estimate and subtract the classical entropy generated by the experimental preparation and imaging processes. The region of the phase diagram near half-filling and small J/U offers rich possibilities that complement the existing experiments at unity-filling and larger J/U [20, 21]. New possible directions such as non-adiabatic preparation (sudden expansion) and the inclusion of fermions are briefly discussed in the conclusions.

II. MODELS

In this section, we remind the definition the O(2) model and explain how it can be quantum simulated with a simple BH model for sufficiently large chemical potential. A more general discussion of the connection between the O(2) and BH models can be found in [25]. The O(2) model shares many features with other abelian LGT models. In 1+1 dimensions, its partition function reads:

$$Z = \int \prod_{(x,t)} \frac{d\theta_{(x,t)}}{2\pi} \mathrm{e}^{-S}, \tag{1}$$

with the action

$$S = -\beta_\tau \sum_{(x,t)} \cos(\theta_{(x,t+1)} - \theta_{(x,t)} - i\mu) \\ -\beta_s \sum_{(x,t)} \cos(\theta_{(x+1,t)} - \theta_{(x,t)}), \tag{2}$$

and sites on a $N_s \times N_\tau$ rectangular lattice labeled (x,t). In LGT, space and Euclidean time are treated on the same footing, a remnant of the Lorentz invariance expected in the continuum limit. For these reasons, it is often considered in the isotropic limit where $\beta_s = \beta_t$. The von Neumann entanglement for the isotropic model has been calculated numerically [26] using tensor Renormalization Group methods [25, 27].

In order to connect the O(2) model with quantum simulators, it is possible to take a highly anisotropic limit $\beta_\tau \gg \beta_s$ of the transfer matrix where the time becomes continuous and we can identify a quantum Hamiltonian [25, 28–31] :

$$\hat{H} = \frac{U}{2} \sum_x \hat{L}_x^2 - \tilde{\mu} \sum_x \hat{L}_x - 2J \sum_{\langle xy \rangle} \cos(\hat{\theta}_x - \hat{\theta}_y) \ , \tag{3}$$

with $[\hat{L}_x, \mathrm{e}^{i\hat{\theta}_y}] = \delta_{xy} \mathrm{e}^{i\hat{\theta}_y}$. These commutation relations can be approximated with finite integer spin [25]. In the following, we use the spin-1 and spin-2 approximations for numerical calculations. This approximation if justified for the regime considered below ($\tilde{\mu} \simeq U/2 \gg J$), where the states with a large angular momentum play an inessential role. Quantum simulators involving two species of bosonic atoms have been proposed for the spin-1 approximation [25, 32]. Note that for reasons explained in the next paragraph, we only consider models with a single species of boson in the rest of the paper. This effort is directly related to recent attempts (for recent reviews see Refs. [33–35]) to develop quantum simulators for models studied in LGT. Note that the non-zero eigenvalues of $\hat{L}$ come in pairs with opposite signs. When $\tilde{\mu} = 0$, the sign of these eigenvalues plays no role and there is an exact invariance under the charge conjugation which implies the existence of anti-particles.

On the other hand, when $\tilde{\mu}$ is large and positive, the states with negative eigenvalues play a minor role in numerical calculations. If we omit these states, we can replace $\hat{L}_x$ by the occupation number n_x and $\mathrm{e}^{i\hat{\theta}_x}$ by the creation operator $a_x^\dagger$ in Eq. (3). We then obtain the simple BH Hamiltonian:

$$\hat{H} = \frac{U}{2} \sum_x n_x(n_x - 1) - J \sum_x (a_x^\dagger a_{x+1} + h.c.). \tag{4}$$

This approximate correspondence already discussed in the literature [30, 31] is supported by results presented below. In the following, we focus on the region of the phase diagram where $\tilde{\mu} \simeq U/2 \gg J$ illustrated in Fig. 1. In this regime, the particle occupancies 0 and 1 dominate for BH (hard core limit) and there is an *approximate*

correspondence with the spin-1/2 XX model which is integrable and has a central charge $c = 1$ [12, 13]. Note that in order to compare with experiment, we have fixed $\tilde{\mu} = U/2$ and we will then work in the canonical approach with a fixed number of particles. In the grand canonical approach, near the tip of the SF phase, the changes in $\tilde{\mu}$ necessary to change the number of particles are very small.

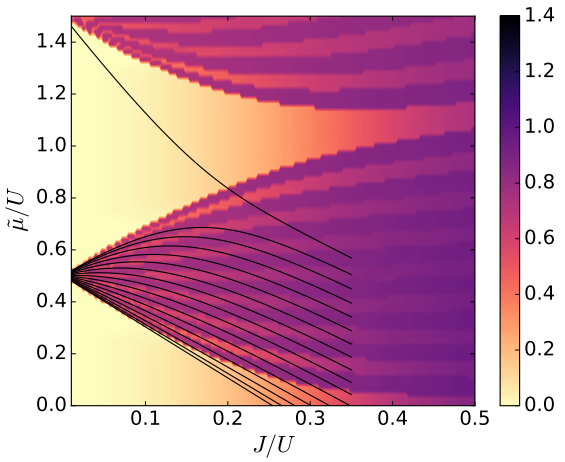

FIG. 1. (color online) S_2 for O(2) with $N_s = 16$ and OBC. Laid over top are the BH boundaries between particle number sectors.

III. THE SECOND-ORDER RÉNYI ENTROPY

Recent cold atom experiments [20, 21] have measured the second-order Rényi entropy

$$S_2(\mathcal{A}) \equiv -\ln(\mathrm{Tr}(\rho_{\mathcal{A}}^2)) \ , \tag{5}$$

for a variety of subsystems $\mathcal{A}$ and open boundary conditions (OBC). The reduced density matrix $\hat{\rho}_{\mathcal{A}}$ is obtained by tracing over the complement of $\mathcal{A}$. CFT provides severe restrictions on the dependence of S_2 on the size of the system and the subsystem [14–17, 36]. In the following, we restrict ourselves to systems with an even number of sites and a subsystem $\mathcal{A}$ of size $N_s/2$. Fits of other subsystems are discussed in in the appendix and in a more detailed study [24]. Fig. 1 displays S_2 for $N_s = 16$ as a function of J/U and the chemical potential. The lower (upper) light part is the Mott phase with particle density $\lambda = 0$ (1), and the 15 plateaus corresponding to the particle number sectors 1, 2, ..., $N_s - 1$ in the SF phase in between are visible. The boundaries of the SF phase, $\tilde{\mu}/U = 1/2 \pm 2J/U$ at small J, follow from a perturbative calculation and are consistent with Refs. [37, 38] for BH at larger J . In the following, we focus on the half-filling region which is more or less horizontal in the SF region and can be reached numerically at arbitrarily small J/U.

Since existing experiments only allow a very limited number of sites, it is crucial to take into account subleading corrections. Using existing results [14–17, 36] for subsystems of size $N_s/2$, we consider the form:

$$S_2(N_s) = K + A\ln(N_s) + \frac{B\cos\left(\frac{\pi N_s}{2}\right)}{(N_s)^p} + \frac{D}{\ln^2(N_s)}, \tag{6}$$

where K, A, p, B, and D are fitting parameters. Of these parameters, only A is universal; however, p is expected to follow certain special relations between p values for the first order Rényi entropy (von Neumann entropy) and the second order Rényi entropy for both open and periodic boundary conditions (see Ref. [24] and references therein). For OBC, the CC scaling predicts $A = c/8$. In order to verify this prediction, we have calculated S_2 at half-filling for $J/U = 0.1$ for the two models considered with the Density Matrix Renormalization Group (DMRG) method [39, 40] using the ITensor C++ library [41] For the O(2) model, the results were cross-checked [24] with tensor Renormalization Group methods [25–27].

If we use the numerical data for N_s up to 64, we obtain $A = 0.1263$ for O(2) and 0.1278 for BH which is close to the CC prediction 0.125 for $c = 1$. The difference between the two models can be reduced significantly by decreasing J/U, which also brings A closer to 0.125 [24]. In order to test the predictive ability of the fit for smaller spatial sizes we have reduced the maximal value N_s^{max} of N_s from 64 to smaller values, down to 12. The results for S_2 and A are shown in Fig. 2 which suggests that the estimates converge slowly to the CFT value as N_s^{max} increases. It has also been noticed that if J/U is increased to $J/U \simeq 0.3$ for BH, the sign of D changes in a way that seems almost independent of the other subleading corrections used. In this region of parameters, the periodic corrections are smaller which may facilitate the estimate of c, however the close connection with the O(2) model is lost.

IV. EXPERIMENTAL SETUP

We now proceed to explain the proposed experimental setup. We consider an optical lattice experiment with single-particle resolved readout and local manipulation of the optical potential, similar to Ref. [20]. In the experiment, two copies of the one-dimensional many-body state of interest are prepared in adjacent rows of an optical lattice, and global and local Rényi entropies can be measured by a beamsplitter operation implemented via a controlled tunneling operation between the two copies (Fig. 3a). The parity of the atom number in one copy after the beamsplitter operation gives access to the quantum mechanical purity [23].

BH systems with tunable parameters U and J and well-defined particle number are realized in current experiments with one particle per site. Fig. 3b shows a proposed scheme to achieve half-filling at $J/U \approx 0.1$:

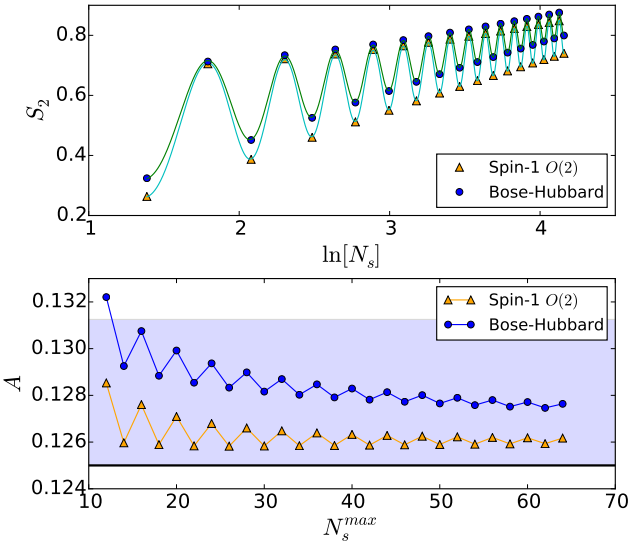

FIG. 2. (color online) (top) S_2 at half-filling with OBC for O(2) and BH with $J/U = 0.1$. The solid lines are the fits for BH and O(2). (bottom) Values of A as a function of the maximal value of N_s used in the fit, the band represents a positive departure of 5 percent from the expected value 0.125.

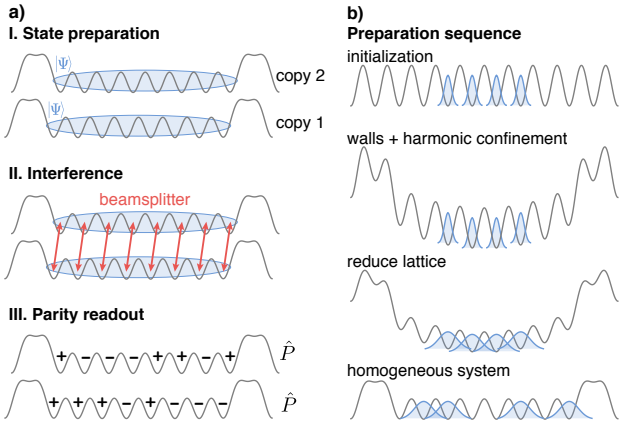

FIG. 3. (color online) Measuring entanglement entropy in optical lattices. a) Two copies of a quantum state $|\Psi\rangle$ interfere under a beamsplitter operation, and site-resolved number measurements reveal the local parity $\hat{P}$ and entanglement entropy. b) Proposed state preparation for BH systems at half-filling, here for 4 atoms on 8 sites. Particles indicated by wavefunctions are initialized in a deep optical lattice, where the local environment can be shaped via harmonic confinement and sharp features projected with a spatial light modulator. As the lattice depth is reduced, the particles delocalize but are confined by repulsive walls.

N_p bosons are initialized in the Mott regime $J \ll U$, as in current experiments. We additionally superimpose a harmonic confinement and two sharp, confining walls separated by N_s sites, which define the boundaries of the system and may be realized using holographic techniques as in Ref. [20]. After the tunneling is increased to the desired value ($J/U \approx 0.1$), we adiabatically remove the harmonic confinement. This step allows the population to smoothly redistribute from the center of the system to the edges and realizes the ground state with uniform density and hard wall boundary conditions. We have verified that for realistic experimental parameters of $U/h = 1\,\mathrm{kHz}$ and $J/h = 100\,\mathrm{Hz}$, the sequence in Fig. 3 b) with $N_s = 8$ requires an adiabaticity time scale of only $\sim 12\,\mathrm{ms}$ and we estimate that even the largest systems with $N_s = 64$ can be prepared in approximately one second. Alternatively, techniques based on optical superlattices may be able to prepare lattice ground states at half-filling [42].

After preparing twin tubes with half-filling in their ground state and applying the beamsplitter operation, one can measure the number of particles modulo 2 at each site x of a given copy (n_x^{copy}) [20], and use the result [23]:

$$\exp(-S_2) = \mathrm{Tr}(\rho_{\mathcal{A}}^2) = \langle (-1)^{\sum_{x\in\mathcal{A}} n_x^{copy}} \rangle \,, \qquad (7)$$

to calculate S_2.

The probability for parity $(-1)^{n_x} = \pm 1$ is $(1 \pm \exp(-S_2))/2$. As S_2 increases, more cancellations occur and one needs on the order of $\exp(2S_2)$ measurements to overcome the fluctuations. From Fig. 2, and assuming N_s to be less than 16 S_2 is of order 0.7 or less. $N_s \leq 16$ means less than eight particles at half-filling. Using the supplementary material of Ref. [21], we estimate that the classical entropy per particle is of order 0.05. For this range of parameters, the maximal measured S_2 is less than 1.1. For $\mathcal{N}$ independent measurements, we find that the statistical error is

$$\sigma_{S_2} = \sqrt{(e^{2S_2} - 1)/\mathcal{N}} \,. \qquad (8)$$

For the maximal value $S_2 = 1.1$, it takes about 800 measurements to reach $\sigma_{S_2} \simeq 0.1$. Due to the logarithmic growth of S_2, the number of measurements only needs to increase like $N_s^{1/4}$ to maintain a desired accuracy, which is not a prohibitive growth.

In addition to the statistical errors, one needs to take into account that finite temperature as well as preparation and manipulation errors contribute a classical entropy $S^{class.}$. Assuming that this classical entropy is linear in the number of particles in the system, it can be estimated by making use of an approximate particle-hole symmetry: near half-filling, $S_2(N_s)$ of the ground state is in good approximation symmetric in the particle number about $N_p = N_s/2$. By measuring $S_2^{exp.}(N_s)$ for a range of particle numbers in the vicinity of $N_s/2$, the excess classical entropy per particle in the experiment can be determined. Subtracting this estimate of the classical entropy from the experimentally measured $S_2^{exp.}$ gives a corrected estimate of the ground state entanglement entropy $S_2^{corr.}$, which we compare to CFT via Eq. (6). For the system sizes considered here, deviations from an exact particle-hole symmetry are small and exhibit a regular behavior at zero and finite temperature [43]. Understanding and fitting these effects is important to get estimates of $S_2^{corr.}$

with errors less than 0.02 [44].

In order to give an idea of possible experimental outcomes, we have numerically studied the sensitivity of the fit results of Eq. (6) to statistical errors in the measured values of S_2. By repeatedly fitting synthetically generated data (SGD) with Gaussian noise on S_2 of magnitude σ_{S_2} as illustrated in Fig. 4 (left), we find that it translates into errors of the fit approximately as $\sigma_A = 3.1\sigma_{S_2}$ for a global fit of the central charge involving data up to $N_s = 16$. To reach a statistical uncertainty in A comparable to systematic errors of the order 0.02, the statistical error on σ_{S_2} has to be on the order of 0.005.

Alternatively, we can try to fit $S^{class.}$. For this purpose, we have considered finite temperature (T) effects in Fig. 4 (left) for $T = 0.2J$ and $0.4J$, which are on the order of temperatures reached in current experiments [45]. Remarkably, these effects can be fitted by adding only one term linear in N_s. If $S^{class.}$ generated during the experiment follows this linear behavior, it may be used to determine some effective temperature. It is shown in the appendix that the finite temperature effects become more important as we decrease J. Note that by including a term linear in the system or sub-system size in the fit to take into account the effects from the thermal entropy, the value of A found in the absence of thermal entropy effects is changed so that the high degree of agreement found between the fit parameter and CFT is lost, regardless of the quality of the fit. In order to maintain the agreement between the CFT prediction for c, and the value of c found by fitting, additional corrections must be included.

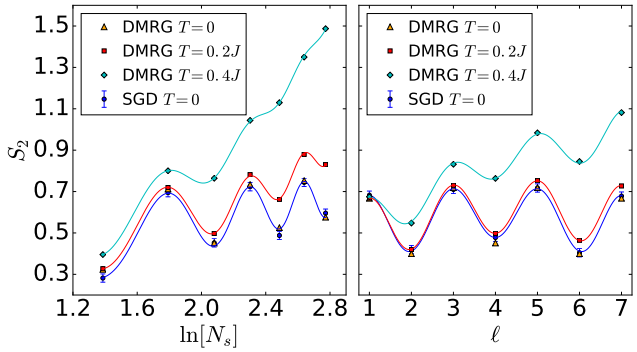

FIG. 4. (color online) S_2 at half-filling for BH with $J/U = 0.1$ and SGD with random Gaussian fluctuations with $\sigma_{S_2} = 0.02$. (left): vs. $\ln(N_s)$ for a subsystem of size $N_s/2$ with the solid line corresponding to a fit of the SGD from Eq. (6). (right): vs. the subsystem size ℓ for $N_s = 8$; the solid line corresponds to a fit of the SGD using the formulas of Ref. [46]. Same quantities for $T = 0.2J$ and $T = 0.4J$.

So far we have only used the values of S_2 corresponding to a subsystem of size $N_s/2$. CFT also provides prediction for arbitrary subsystem sizes ℓ with $1 \leq \ell \leq N_s - 1$ which are described in the appendix. The large oscillations when ℓ is changed for $N_s = 8$ are shown in Fig. 4 (right). Finite-T effects can be fitted with a single additional term linear in ℓ. Importantly, the experimental measurements of the parities at each site shown in Eq. (7) allow us to calculate S_2 for *all* possible subsystems without extra measurements. Estimates of c from numerical calculations at fixed N_s fits in other models have up to 20 percent errors [24, 47]. Knowing S_2 for all the subsystems also allows us to calculate the mutual information [18, 20], where the $S^{class.}$ contributions cancel.

V. CONCLUSIONS

In conclusion, we have shown that the simple BH model which is implemented in current experimental measurements of S_2 can be used as a quantum simulator for the classical O(2) model with a chemical potential. We showed that the region of the phase diagram near half-filling and small J/U offers rich possibilities that complement the existing experiments at unity-filling and larger J/U [20, 21]. The changes in S_2 due to the size of the system or the subsystem show strong periodic oscillations which are of the same order of magnitude as the average S_2 for $N_s \leq 16$. We provided complementary methods to estimate and subtract $S^{class.}$ from $S_2^{exp.}$. Existing experiments could immediately confirm the periodic patterns found in the numerical calculations and fits. Accurate determination of c would require larger statistics or a suitable use of the complete information about the subsystems. Conformal symmetry connects disparate physical systems from condensed matter and LGT. While this equivalence is usually apparent in theory in the thermodynamic limit, we have shown that the basic equivalence between the BH model and the classical O(2) model can already be identified in present cold-atom experiments. Our proposed method could enable the first direct verification of conformal scaling in an experimentally accessible system.

New directions should be pursued. Half-filling initial states can also be obtained by a sudden expansion. The presence of additional approximate conserved charges makes the thermalization non-trivial and interesting [48–51]. The possibility of revivals in the time-dependent $S_2(t)$ for time scales of the order of 200 ms for $J/U = 0.1$, a duration about 10 times longer than current experiments [21], is under study. The techniques discussed here for the bosonic case can also be applied to Fermi-Hubbard systems [18], for which optical lattice experiments with single-site resolution are rapidly becoming available [52–55]. It would be desirable to develop specific procedures to study models with other values of c (Ising, Z_N clock, Potts) or with $O(3)$ symmetry with a chemical potential, which have a similar phase diagram [56], and could be quantum simulated [57]. More insight on conformal symmetry could be gained by studying particle number fluctuations [58–60]. The entanglement entropy can also be calculated in pure gauge theories using standard Monte Carlo methods [61]. Methods for calculating the entanglement entropy in the presence of fermion determinants

have been designed on the lattice [62] and in the continuum [63].

Appendix: Fits of S_n

This appendix aims to provide background calculations done for the Bose-Hubbard (BH) and O(2) model that give empirical evidence to the claims made in the main text. The main text put forward that in the right region of coupling space (i.e. small enough hopping J relative to the on-site repulsion, U) at half-filling, it is possible to quantum simulate the O(2) model using a single species Bose-Hubbard model, and in said simulation, measure the Rényi entanglement entropy and subsequently the conformal central charge, c. We considered the BH and O(2) models at half-filling, however in this appendix the O(2) model only makes an appearance in Fig 5.

The choice for half-filling was made because of the following: Near the boundaries of the Mott insulator lobes with the superfluid phase the Rényi entropy takes on a constant value of $\ln(2)$. Between each lobe there are $N_s - 2$ boundaries denoting the particle number in the chain, with an approximate symmetry around $N_s/2$ particles (i.e. half-filling for bosons). This number has the clearest signal for the entanglement entropy (see Ref. [24]) and therefore all work here, and in the main text, was done at half-filling. In addition, all work here and in the main text was done with open boundary conditions. However, while this is more easily realized in experiment, the second order Rényi entropy with open boundary conditions has much larger fluctuations than the von Neumann entropy (See Ref. [24]).

Here we first consider fits to the second order Rényi entanglement entropy, S_2, across a range of J/U values to better understand the dependence on J/U. Next we consider fits made to data across the entire range of system sizes, N_s, and across all subsystem sizes, l. These fits span the entire N_s-l plane and aim to explain how we decided to specifically focus on the case $l = N_s/2$. We report the average relative error for fits to large and small systems. We mention some investigation into taking finite temperature effects into account in experiments. Finally we discuss how we used synthetic Gaussian fluctuations to simulate errors on experimental data and estimate the error that would be incurred on measuring the central charge.

In order to understand how the fits were influenced by J/U, we considered fits of S_2 across a range of J/U values. These fits were done with DMRG data for $N_s = 4$ up to $N_s = 64$. We fit the second order Rényi entanglement entropy with a subsystem size of $l = N_s/2$ and compared the coefficient of logarithmic scaling, A, between the BH and O(2) models for various finite-size correction terms. The A values as a function of J/U can be found in Fig. 5 with a correction term proportional to $1/\ln^2(N_s)$ which is predicted by conformal field theory (CFT) [17]. We considered additional corrections like $1/N_s$, $1/\ln(N_s)$, etc

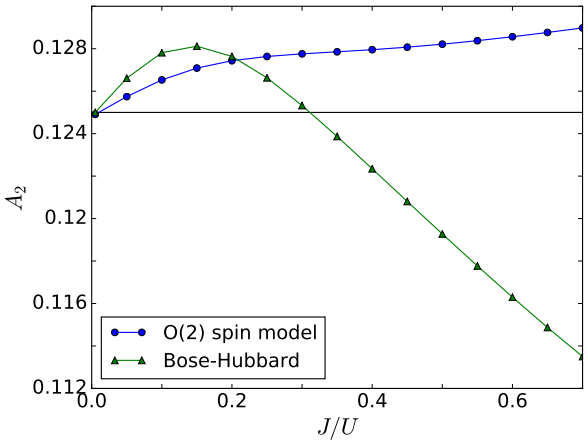

FIG. 5. (color online) The A values from fits to S_2 with open boundary conditions for Bose-Hubbard data and O(2) spin model data with a spin-1 truncation at half-filling. The horizontal line is the conformal field theory prediction. The A values were extracted from a fit to Eq. A.1 with a correction term proportional to $1/\ln^2(N_s)$. The farthest point to the left is at $J = 0.005$, and the lines through the data are meant to guide the eye.

... We found some features were robust across different functional forms for the corrections. For larger J/U the BH A values tended to decrease monotonically, while the O(2) A values seem to increase. There appears to be a crossing between the BH data and the CFT prediction around $J/U \approx 0.35$. However at small J/U, only the correction $\propto 1/\ln^2(N_s)$ showed a tendency towards $A_2 \approx 1/8$ as $J/U \to 0$, a soluble limit where $c = 1$. The choice for $J/U = 0.1$ for quantum simulation is a nice compromise since ideally the smaller the J/U the better for the mapping between BH and O(2), however, for experimental purposes too small a value of J is inconvenient because of the associated long time scales and sensitivity to uncontrolled disorder, and finite temperature effects are larger at smaller J/U.

At this point, it's important to reiterate that calculations done in the rest of this text specifically refer to the BH model. A deeper investigation into the O(2) spin model can be found in Ref. [24].

CFT gives predictions for the scaling of the Rényi entropy as a function of subsystem size. Eq. A.1 gives the leading order prediction along with a term believed to account for finite-size effects and parity oscillations [46]. Importantly, the experimental measurements of the parities at each site shown in Eq. 7 in the main text allow us to calculate S_2 for all possible subsystems without extra measurements. The possibility of using these additional (but statistically correlated) results to reduce the overall statistical error on the estimate is under study.

We explored S_2 as a function of system size, N_s, and subsystem size, l, in the BH model. As an example we have the subsystem data plotted for two different system

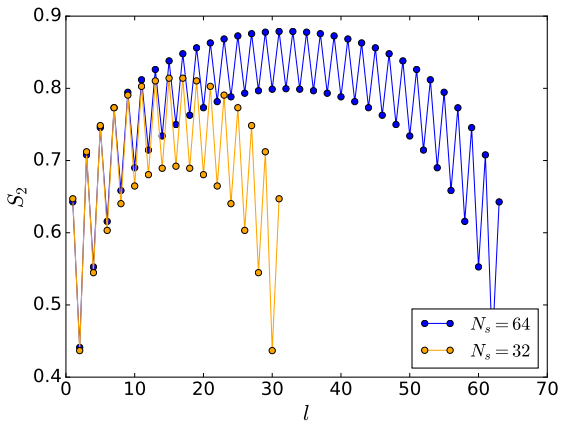

FIG. 6. (color online) S_2 for the Bose-Hubbard model at $J/U = 0.1$, with open boundary conditions. Here the data from $N_s = 32$ and 64 is plotted together as an example of the oscillatory behavior of the data as a function of the subsystem size, l.

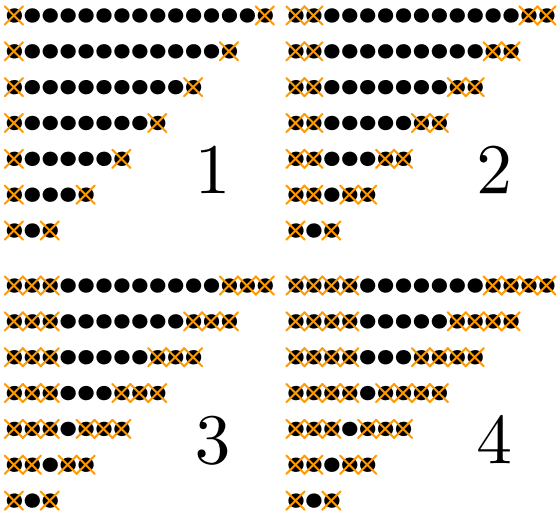

FIG. 7. How points are removed when preforming a global fit to the entire data set to determine the influence of the boundary points on the average relative error. Here the system size increases in the vertical direction (N_s), and the subsystem size increases in the horizontal direction (l). The first four steps are shown.

sizes, $N_s = 32$ and 64, in Fig. 6. From the plot one can see that for small l and $l \approx N_s$, the amplitudes are almost independent of N_s, however near $l \approx 12$ the data sets depart. We attempted fits using

$$S_n(N_s, l) = A_n \ln\left\{N_s \sin\left[\frac{\pi l}{N_s}\right]\right\} + B + \frac{C}{N_s^{p_n}} \cos(\pi l) \left|\sin\left[\frac{\pi l}{N_s}\right]\right|^{-p_n} + f_n(N_s, l) \tag{A.1}$$

as well as including the order $1/l$ corrections [46],

$$S_n(N_s, l) = A_n \ln\left\{\frac{4(N_s+1)}{\pi} \sin\left[\frac{\pi(2l+1)}{2(N_s+1)}\right]\right\} + B + \frac{C}{N_s^{p_n}} \cos(\pi l) \left|\sin\left[\frac{\pi(2l+1)}{2(N_s+1)}\right]\right|^{-p_n} + f'_n(N_s, l) \tag{A.2}$$

where f'_n and f_n are correction terms. We performed global fits across the entire N_s-l plane in order to take full advantage of the data.

The largest discrepancies between the fit and the data appear at small N_s, with discrepancies remaining on the boundary (small l and $l \approx N_s$) and lesser error near the center of the chain at larger values of N_s. We then considered the removal of points from the boundary (points from small l and $l \approx N_s$) in the pattern shown in Fig 7. When fitting to the entire data set we first remove a single point from the left and right (1 and $N_s - 1$) and perform a fit. Starting over, we then remove a single point from $N_s = 4$ on both sides, but two points from all larger N_s and perform a fit. Starting yet again we remove a single point from both sides for $N_s = 4$, two points from both sides for $N_s = 6$, and three points from either side for all larger N_s and perform a fit. We continue this until only the center points from $N_s/2$ remain. This allows us to identify the contributions to the error from the points away from the center of the chain.

In order to measure the error on the fits we used the average relative error

$$(\text{Relative Error})^2 = \frac{1}{N} \sum_{i=0}^{N-1} \left(\frac{y_i - f(x_i)}{y_i}\right)^2 \tag{A.3}$$

for N data points, with y_i the dependent data, x_i the independent data, and f the fit. This measure has the advantage of being dimensionless. The average relative error for two examples of $N_s = 64$ and 16 is found in Fig. 8. In this Figure we see for small N_s (right) that as the maximum number of points removed following the procedure above, n_r^{max}, approaches $N_s/2 - 1$ the relative error takes a minimum. We see the optimum fit for the entire data set (left) takes place when all points except the center ones have been removed for small N_s, and a "fan" of points remain for larger N_s. When considering fits with f and $f' \neq 0$ we again tried various, typical functional forms. These included corrections $\propto 1/N_s$, $1/N_s^2$, and $1/\ln(N_s)$ as well as corrections from [64]. All of these corrections obtained similar relative errors.

We considered the effects of a finite temperature for a few cases on the Rényi entropy. An example of the finite temperature effects on the scaling with the system size is shown in Fig. 9. As one can see the finite temperature effects are much more pronounced for smaller J/U. To take the finite temperature effects into account it is

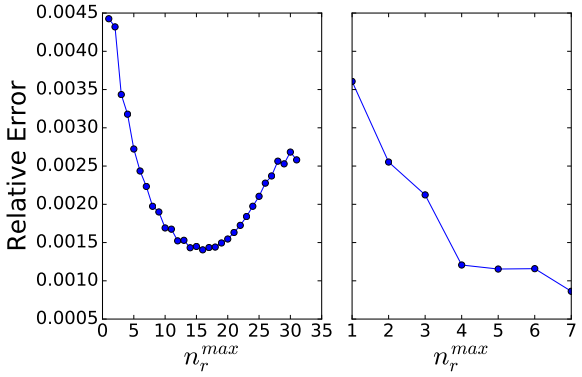

FIG. 8. The average relative error versus the maximum number of points removed (n_r^{max}) from the boundary during the fit. (left) Fitting to the entire data set, $4 \leq N_s \leq 64$, we see the optimum fit occurs when the majority of the smaller N_s data has been removed except for the center points. However a "fan" of data remains for the larger N_s data. (right) Fitting data such that $4 \leq N_s \leq 16$. From this we see the optimum fit occurs particularly at $l = N_s/2$.

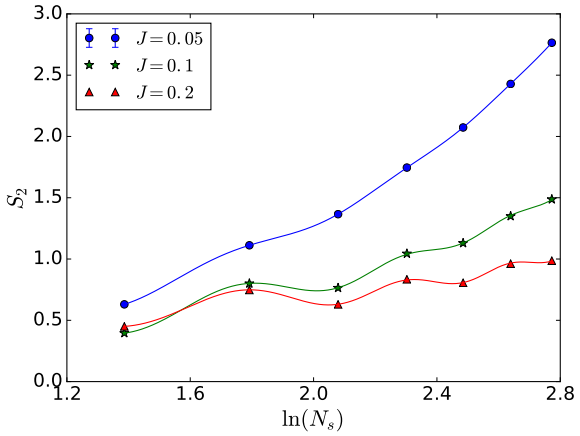

FIG. 9. (color online) The second order Rényi entropy, S_2, as a function of the logarithm of system size with a finite temperature and $l = N_s/2$. Here $U = 1$ and $T = 0.04$ is shown. The lines through the data points are fits using Eq. A.1 with one addition term linear in the system size. The $J = 0.05$ data used sampling methods however the errors are smaller than the markers.

enough to add a term linear in l or N_s, for the subsystem or system scaling respectively. The fits in Fig. 9 and those used in the main text were done similarly, using Eq. A.1 with an additional linear term.

It is possible to investigate the influence of statistical fluctuations of the pure $T = 0$, S_2 data. This can be accomplished by adding Gaussian fluctuations drawn from a distribution with a specified σ_{S_2}. This synthetic data mimics the actual experimental results under the assumption that the error associated with each data point is the same regardless of system size or subsystem size.

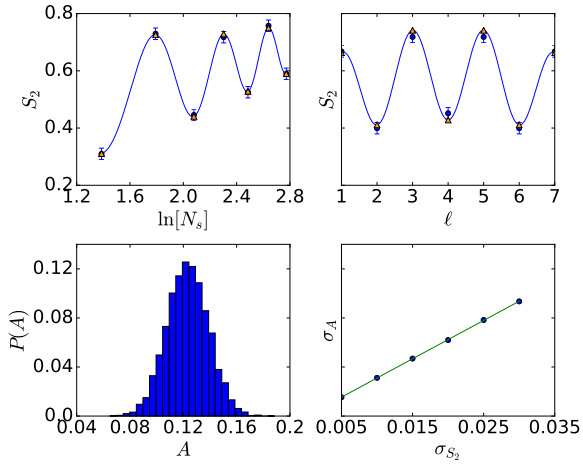

FIG. 10. (color online) (top-left) S_2 with open boundary conditions at $T = 0$ and the same data with added Gaussian fluctuations as a function of $\ln[N_s]$ with a fit to the fluctuating data. (top-right) S_2 with open boundary conditions as a function of subsystem size for a fixed system size of $N_s = 8$. (bottom-left) The probability distribution for A values extracted from fits to fluctuating data. This distribution was built from 10,000 "experiments". (bottom-right) The error on the mean A values extracted from fits to the fluctuating data versus the error on S_2. The blue circles are the data, while the solid line is a linear fit with slope ≈ 3.1.

By running many "experiments" one can see, approximately, how many measurements are needed for a given single experiment to obtain acceptable results.

To do this, one takes the pure, $T = 0$ data and adds Gaussian noise with σ_{S_2} to the data and then fits the data to the desired functional fit. One does this many times and bins the fit parameters to obtain a histogram of the fit parameters for many experiments. With the histogram one can extract σ_A, the error on the measurement of the central charge. In addition one can establish the relationship between σ_{S_2} and σ_A to understand the size of the errors necessary on S_2 to obtain reliable estimates of c. In Fig. 10 one can see how the addition of Gaussian fluctuations modifies the data and the estimates of c. Using the distribution of A values obtained from the fits we can extract σ_A. In addition we can repeat this again for a different σ_{S_2}. By doing this we find an approximately linear relationship between σ_A and σ_{S_2}, such that $\sigma_A \approx 3.1\sigma_{S_2}$. For a systematic error of 0.02 on the measurement of A, the uncertainty in S_2 must be approximately 0.006. This gives an estimate on the number of measurements necessary, assuming a maximum entropy of 1.1. Using Eq. (6) in the main text we find on the order of 193,000 measurements.

ACKNOWLEDGMENTS

Acknowledgments. We thank M. C. Banuls, I. Bloch, I. Cirac, M. Greiner, A. Kaufman, G. Ortiz, J. Osborn, H. Pichler and P. Zoller for useful suggestions or comments. This research was supported in part by the Department of Energy under Award Numbers DOE grant DE-FG02-05ER41368, DE-SC0010114 and DE-FG02-91ER40664, the NSF under grant DMR-1411345 and by the Army Research Office of the Department of Defense under Award Number W911NF-13-1-0119. L.-P. Yang was supported by Natural Science Foundation for young scientists of China (Grants No.11304404) and Research Fund for the Central Universities(No. CQDXWL-2012-Z005). P.M.P. has received funding from the European Union's Horizon 2020 research and innovation programme under the Marie Sklodowska-Curie grant agreement No 706487. Parts of the numerical calculations were done at the Argonne Leadership Computational Facilities. Y.M. thanks the Focus Group Physics with Effective Field Theories of the Institute for Advanced Study, Technische Universität München, and the workshop on "Emergent properties of space-time" at CERN for hospitality while part of this work was carried out and the Institute for Nuclear Theory for motivating this work during the workshop "Frontiers in Quantum Simulation with Cold Atoms".

[1] A. M. Polyakov, *Gauge Fields and Strings*, Contemporary concepts in physics (Taylor & Francis, 1987), ISBN 9783718603930.

[2] P. Di Francesco, P. Mathieu, and D. Sénéchal, *Conformal field theory*, Graduate texts in contemporary physics (Springer, New York, NY, 1997).

[3] A. A. Belavin, A. M. Polyakov, and A. B. Zamolodchikov, Nucl. Phys. **B241**, 333 (1984).

[4] D. Friedan, Z.-a. Qiu, and S. H. Shenker, Phys. Rev. Lett. **52**, 1575 (1984).

[5] V. S. Dotsenko, Nucl. Phys. **B235**, 54 (1984).

[6] S. El-Showk, M. F. Paulos, D. Poland, S. Rychkov, D. Simmons-Duffin, and A. Vichi, Phys. Rev. D **86**, 025022 (2012).

[7] T. DeGrand, Phil. Trans. R. Soc. A **369**, 2701 (2011), 1010.4741.

[8] J. Kuti, PoS **KMI2013**, 002 (2015).

[9] V. L. Berezinskiĭ, Soviet Journal of Experimental and Theoretical Physics **32**, 493 (1971).

[10] J. M. Kosterlitz and D. J. Thouless, Journal of Physics C Solid State Physics **6**, 1181 (1973).

[11] D. B. Kaplan, J.-W. Lee, D. T. Son, and M. A. Stephanov, Phys. Rev. **D80**, 125005 (2009), 0905.4752.

[12] G. Vidal, J. I. Latorre, E. Rico, and A. Kitaev, Physical Review Letters **90**, 227902 (2003), quant-ph/0211074.

[13] V. E. Korepin, Phys. Rev. Lett. **92**, 096402 (2004).

[14] P. Calabrese and J. L. Cardy, J.Stat.Mech. **0406**, P06002 (2004), hep-th/0405152.

[15] P. Calabrese and J. L. Cardy, Int.J.Quant.Inf. **4**, 429 (2006), quant-ph/0505193.

[16] P. Calabrese, M. Campostrini, F. Essler, and B. Nienhuis, Phys. Rev. Lett. **104**, 095701 (2010).

[17] J. Cardy and P. Calabrese, Journal of Statistical Mechanics: Theory and Experiment **2010**, P04023 (2010).

[18] H. Pichler, L. Bonnes, A. J. Daley, A. M. Läuchli, and P. Zoller, New Journal of Physics **15**, 063003 (2013), 1302.1187.

[19] L. Bonnes, H. Pichler, and A. M. Läuchli, Phys. Rev. B **88**, 155103 (2013).

[20] R. Islam, R. Ma, P. M. Preiss, M. E. Tai, A. Lukin, M. Rispoli, and M. Greiner, Nature **528**, 77 (2015).

[21] A. M. Kaufman, M. E. Tai, A. Lukin, M. Rispoli, R. Schittko, P. M. Preiss, and M. Greiner, Science **353**, 794 (2016).

[22] C. Moura Alves and D. Jaksch, Phys. Rev. Lett. **93**, 110501 (2004).

[23] A. J. Daley, H. Pichler, J. Schachenmayer, and P. Zoller, Phys. Rev. Lett. **109**, 020505 (2012).

[24] A. Bazavov, Y. Meurice, S. W. Tsai, J. Unmuth-Yockey, L.-P. Yang, and J. Zhang (2017), arXiv:1703.10577, submitted to Phys. Rev. D.

[25] H. Zou, Y. Liu, C.-Y. Lai, J. Unmuth-Yockey, L.-P. Yang, A. Bazavov, Z. Y. Xie, T. Xiang, S. Chandrasekharan, S.-W. Tsai, et al., Phys. Rev. A **90**, 063603 (2014).

[26] L.-P. Yang, Y. Liu, H. Zou, Z. Y. Xie, and Y. Meurice, Phys. Rev. E **93**, 012138 (2016).

[27] Y. Liu, Y. Meurice, M. P. Qin, J. Unmuth-Yockey, T. Xiang, Z. Y. Xie, J. F. Yu, and H. Zou, Phys. Rev. **D88**, 056005 (2013), 1307.6543.

[28] E. Fradkin and L. Susskind, Phys. Rev. D **17**, 2637 (1978).

[29] J. B. Kogut, Rev. Mod. Phys. **51**, 659 (1979).

[30] M. P. A. Fisher, *Strong Interaction in Low Dimensions* (Kluwer Academic, 2004).

[31] S. Sachdev, *Quantum phase transitions* (Cambridge University Press, 2011), second ed. ed., ISBN 9780521514682.

[32] A. Bazavov, Y. Meurice, S.-W. Tsai, J. Unmuth-Yockey, and J. Zhang, Phys. Rev. D **92**, 076003 (2015).

[33] L. Tagliacozzo, A. Celi, A. Zamora, and M. Lewenstein, Annals Phys. **330**, 160 (2013), 1205.0496.

[34] U.-J. Wiese, Annalen Phys. **525**, 777 (2013), 1305.1602.

[35] E. Zohar, J. I. Cirac, and B. Reznik, Rept. Prog. Phys. **79**, 014401 (2016), 1503.02312.

[36] M. Fagotti and P. Calabrese, Journal of Statistical Mechanics: Theory and Experiment **2011**, P01017 (2011).

[37] G. G. Batrouni and R. T. Scalettar, Phys. Rev. B **46**, 9051 (1992).

[38] T. D. Kühner and H. Monien, Phys. Rev. B **58**, R14741 (1998).

[39] S. R. White, Phys. Rev. Lett. **69**, 2863 (1992).

[40] S. Östlund and S. Rommer, Phys. Rev. Lett. **75**, 3537 (1995).

[41] Version 2.7.10, `http://itensor.org/`.

[42] S. Trotzky, Y.-A. Chen, I. P. McCulloch, U. Schollwöck, J. Eisert, and I. Bloch, Nat. Phys. **8**, 325 (2012).

[43] J. Cardy and C. P. Herzog, Phys.Rev.Lett. **112**, 171603 (2014), 1403.0578.

[44] Jin Zhang et al., work in progress.
[45] A. Mazurenko, C. S. Chiu, G. Ji, M. F. Parsons, M. Kanasz-Nagy, R. Schmidt, F. Grusdt, E. Demler, D. Greif, and M. Greiner, Nature **545** (2017).
[46] J. C. Xavier and F. C. Alcaraz, Phys. Rev. B **83**, 214425 (2011).
[47] L. Mazza, D. Rossini, R. Fazio, and M. Endres, New Journal of Physics **17**, 013015 (2015).
[48] H. Pichler, A. J. Daley, and P. Zoller, Phys. Rev. A **82**, 063605 (2010).
[49] A. J. Daley, Advances in Physics **63**, 77 (2014), 1405.6694.
[50] J. Schachenmayer, L. Pollet, M. Troyer, and A. J. Daley, ArXiv e-prints (2014), 1408.1041.
[51] L. Vidmar, S. Langer, I. P. McCulloch, U. Schneider, U. Schollwöck, and F. Heidrich-Meisner, Phys. Rev. B **88**, 235117 (2013).
[52] E. Haller, J. Hudson, A. Kelly, D. A. Cotta, B. Peaudecerf, G. D. Bruce, and S. Kuhr, Nat. Phys. **11**, 738 (2015).
[53] A. Omran, M. Boll, T. A. Hilker, K. Kleinlein, G. Salomon, I. Bloch, and C. Gross, Phys. Rev. Lett. **115**, 263001 (2015).
[54] L. W. Cheuk, M. A. Nichols, M. Okan, T. Gersdorf, V. V. Ramasesh, W. S. Bakr, T. Lompe, and M. W. Zwierlein, Phys. Rev. Lett. **114**, 193001 (2015).
[55] M. F. Parsons, F. Huber, A. Mazurenko, C. S. Chiu, W. Setiawan, K. Wooley-Brown, S. Blatt, and M. Greiner, Phys. Rev. Lett. **114**, 213002 (2015).
[56] F. Bruckmann, C. Gattringer, T. Kloiber, and T. Sulejmanpasic (2016), 1607.02457.
[57] C. Laflamme, W. Evans, M. Dalmonte, U. Gerber, H. Meja-Daz, W. Bietenholz, U. J. Wiese, and P. Zoller, Annals Phys. **370**, 117 (2016), 1507.06788.
[58] C.-L. Hung, X. Zhang, N. Gemelke, and C. Chin, Nature (London) **470**, 236 (2011), 1009.0016.
[59] S. Rachel, N. Laflorencie, H. F. Song, and K. Le Hur, Phys. Rev. Lett. **108**, 116401 (2012).
[60] T. Fukuhara, S. Hild, J. Zeiher, P. Schauß, I. Bloch, M. Endres, and C. Gross, Phys. Rev. Lett. **115**, 035302 (2015).
[61] P. V. Buividovich and M. I. Polikarpov, Nucl. Phys. **B802**, 458 (2008), 0802.4247.
[62] J. E. Drut and W. J. Porter, Phys. Rev. B **92**, 125126 (2015).
[63] I. R. Klebanov, S. S. Pufu, S. Sachdev, and B. R. Safdi, JHEP **05**, 036 (2012), 1112.5342.
[64] J. C. Xavier and F. C. Alcaraz, Phys. Rev. B **85**, 024418 (2012).